THE JOURNAL OF BIOLOGICAL CHEMISTRY VOL. 285, NO. 29, pp. 22318–22327, July 16, 2010

Novel Derivative of Benzofuran Induces Cell Death Mostly by G2/M Cell Cycle Arrest through p53-dependent Pathway but Partially by Inhibition of NF-κB*

Received for publication, April 8, 2010, and in revised form, May 12, 2010 Published, JBC Papers in Press, May 14, 2010, DOI 10.1074/jbc.M110.131797

Sunil K. Manna[‡1,2], Julie S. Bose[§1], Vijay Gangan[§], Nune Raviprakash[‡], Thota Navaneetha[‡], Pongali B. Raghavendra[¶], Banaganapalli Babajan[¶], Chitta S. Kumar[¶], and Swatantra K. Jain[‖]

From the [‡]Laboratory of Immunology, Centre for DNA Fingerprinting and Diagnostics, Nampally, Hyderabad 500 001, India, [§]Reliance Life Sciences Pvt. Ltd., Mumbai 400701, India, the [¶]Department of Biochemistry, Sri Krishnadevaraya University, Anantapur 515003, India, and the [‖]Department of Biotechnology, Jamia Hamdard, New Delhi 110062, India

The *Dracaena* resin is widely used in traditional medicine as an anticancer agent, and benzofuran lignan is the active component. In this report, we provide evidence that the synthetic derivative of benzofuran lignan (Benfur) showed antitumor activities. It induced apoptosis in p53-positive cells. Though it inhibited endotoxin-induced nuclear factor κB (NF-κB) activation in both p53-positive and -negative cells, the activation of caspase 3 was observed in p53-positive cells. It showed partial cell death effect in both p53-positive and -negative cells through inhibition of NF-κB. Cell cycle analysis using flow cytometry showed that treatment with this novel benozofuran lignan derivative to Jurkat T-cells, but not U-937 cells, resulted in a G2/M arrest in a dose- and time-dependent manner. It increased amounts of p21, p27, and cyclin B, but not phospho-Rb through p53 nuclear translocation in Jurkat T-cells, but not in U-937 cells. It inhibited amounts of MDM2 (murine double minute 2) by repressing the transcription factor Sp1, which was also proved *in silico*. It induced cell death in tumor cells, but not in primary T-cells. Overall, our data suggest that Benfur-mediated cell death is partially dependent upon NF-κB, but predominantly dependent on p53. Thus, this novel benzofuran lignan derivative can be effective chemopreventive or chemotherapeutic agent against malignant T-cells.

The majority of the chemotherapeutic agents presently used for cancer treatment are developed by simple screening for cell growth inhibition assay without knowing the mechanism of their action. Even chemotherapy becomes useless when cells become resistant against those drugs. Thus, understanding of the mechanism of action would be helpful in multiple ways to design many drugs in combination chemotherapy; low concentration of drugs that give better results with lower side effects and to administer alternative drugs for chemotherapy. Such drugs inhibit the growth of a variety of cancer cells by utilizing diverse mechanisms that include cell cycle arrest, induction of apoptosis, disruption of microtubules, inhibition of angiogenesis, and/or increasing oxidative damage (1).

Apoptosis is the consequence of a series of precisely regulated events that are frequently altered in tumor cells. Apoptotic stimuli induce a variety of genes involved in the promotion or inhibition of apoptosis by modulating cell cycle by targeting G2/M checkpoint (2–4). Cyclin B1 often expresses during G2 phase, translocates to the nucleus during early mitosis, and degrades toward the end of mitosis (5). The protooncogenes, *p53* (tumor suppressor gene), *Bcl-2* (antiapoptotic gene), and *Bax-α* (proapoptotic gene), are a class of such genes known to regulate cell cycle and apoptosis (6). Expression of Bcl-2 and Bax is transcriptionally regulated by p53 (7). Bcl-2 expression is also regulated by nuclear factor κB (NF-κB)[3] (8). Furthermore, the *p53* gene is involved in regulation of cell cycle specifically at G2/M arrest and expression of the apoptosis-associated genes (9–11). The murine double minute 2 (MDM2) is a key component of p53 signaling pathway. MDM2 is expressed by transcriptional activation of p53 (12) and Sp1 (13). MDM2 again regulates the amount of p53 by targeting p53 for ubiquitin-mediated degradation (14, 15). MDM2 induces expression of p65 (RelA) through activation of Sp1 (16).

Sangre de drago (dragon's blood), blood-red latex produced by various South American Croton species, is widely used in traditional medicine as an anticancer agent. 3′,4-di-*O*-methylcedrusin or 3-[2-(3,4-dimethoxyphenyl)-3-hydroxymethyl-7-methoxy-2,3-dihydro-1-benzofuran-5-yl]propan-1-ol 5 is one of the naturally occurring active principals of latex and has been used as an inhibitor of tumor cell proliferation (17, 18). A dihydrobenzofuran lignan derivative has been identified as a potential antiproliferative and antitumor agent (19). Precursors and analogues of benzofuran lignan derivatives were synthesized and explored for their potential anti-angiogenic and anti-tubu-

* This work was supported by the Department of Biotechnology (DBT), Government of India.

[1] Both authors contributed equally to this work.

[2] To whom correspondence should be addressed: Immunology, Centre for DNA Fingerprinting & Diagnostics, Nampally, Hyderabad 500 076, India. Tel.: 011-91-40-24749412; Fax: 011-91-40-24749448; E-mail: manna@cdfd.org.in.

[3] The abbreviations used are: NF-κB, nuclear factor κB; CE, cytoplasmic extract; NE, nuclear extract; FITC, fluorescein isothiocyanate; IκBα, inhibitory subunit of NF-κB; IκBα-DN, IκBα dominant negative; MDM, murine double mutant; MFI, mean fluorescence intensity; MTT, 3-(4,5-dimethyl-2-thiozolyl)-2,5-diphenyl-2H-tetrazolium bromide; MUP, methyl umbelliferyl phosphate; PARP, poly(ADP-ribose) polymerase; Rb, retinoblastoma; SA-LPS, serum-activated lipopolysaccharide; SEAP, secretary alkaline phosphatase; PBS, phosphate-buffered saline; EMSA, electrophoretic mobility shift assay; FACS, fluorescent-activated cell sorting; DAPI, 4′,6-diamidino-2-phenylindole; PDB, Protein Data Bank; RMSD, root mean square deviation.

lin/anti-mitotic activities (19). In the current study, we report the discovery of a novel benzofuran lignan, 5-{(*E*)-2-carboxyvinyl}-2-(4-hydroxy-3-methoxyphenyl)-7-methoxy-2,3-dihydro-1-benzofuran-3-carboxylic acid (designated as Benfur), as a potent antimitotic agent and inducer of apoptosis. We report here, for the first time, that this novel benzofuran efficiently arrests Jurkat T lymphocytes ($p53^{+/+}$) in the G2/M phase of the cell cycle and induces apoptosis, thus inhibiting cell growth. Benfur shows differential behavior in cells with different *p53* status. Together it may indicate that the Benfur might be an efficient chemotherapeutic agent against cancer. Possibly *p53* function is required to observe the maximum response exerted via G2/M arrest. Benfur also interacts with Sp1 transcription factor thereby decreasing MDM2 expression and in turn stabilizing the p53. However it also shows partial cell death activity in U937 cells possibly by inhibition of NF-κB, suggesting a *p53*-independent mechanism.

EXPERIMENTAL PROCEDURES

Materials—All synthetic chemicals were obtained from commercial sources. Lipopolysaccharide (LPS), propidium iodide (PI), MTT, 4-methyl umbelliferyl phosphate (4-MUP), caspase 3 substrate (Ac-DVED-pNA), caspase 8 substrate (Ac-ITED-pNA), DMSO, and anti-tubulin antibody were obtained from Sigma Aldrich Chemicals. Penicillin, streptomycin, neomycin, RPMI 1640, Iscove's modified Dulbecco, DMEM medium, and fetal bovine serum, were obtained from Invitrogen (Grand Island, NY). Anti-PARP-FITC conjugate was purchased from Novus Biologicals (Littleton, CO). DAPI and anti-rabbit IgG conjugated with horseradish peroxidase and Alexa Fluor were obtained from Molecular Probes (Eugene, OR). Antibodies against cytochrome *c*, Bcl-2, IκBα, p53, p65, p21, p27, cyclin B, CRM1, MDM2, retinoblastoma (Rb), and phospho-Rb and gel shift oligonucleotides for NF-κB, Sp1, Oct1, and p53 were obtained from Santa Cruz Biotechnology (Santa Cruz, CA).

Cell Lines—The cell lines used in this study were as follows: Jurkat E6.1 TIB-152 (human T cell leukemia), MCF-7 (human breast cancer cell line), U-937 (human histiocytic lymphoma), HeLa (human cervical cancer cell line), K562 (human myeloid leukemia), and HT29 and HCT116 (human colon carcinoma) were obtained from American Type Culture Collection (Manassas, VA). HCT116 cells were stably transfected with the *p53* construct (HCT116 $p53^{+/+}$) and maintained in the laboratory. T-cells were isolated from fresh human blood by the Ficoll-hypaque method. PBMC layer was used, and T-cell population was isolated by removing adherent cells (monocytes/macrophages) and a nylon wool column (B-cells) as described previously (20).

Chemical Synthesis and Characterization of the Novel Benzofuran Lignan Compound—Dimer of methyl ferulate methyl (*E*)-3-[2-(4-hydroxy-3-methoxyphenyl)-7-methoxy-3-methoxycarbonyl-2,3-dihydro-1-benzofuran-5-yl]prop-2-enoate was prepared according to the method of Lemière *et al.* (18). Briefly, ferulic acid methyl ester was dimerized in the presence of silver oxide, dry benzene, and acetone. After evaporation, the residual red brown oil was purified by column chromatography with ethyl acetate-hexane as eluent to produce a white compound. The obtained compound was taken in dichloromethane and treated with tribromide for 2 h at 0 °C. The reaction mixture was decomposed by adding water. The organic layer was washed with a saturated solution of sodium bicarbonate, water, brine, and kept over anhydrous sodium sulfate to yield a concentrated crude mass. This crude mass was further purified by radial chromatography with increasing concentrations of ethyl acetate in petroleum ether to yield a viscous yellow mass as 5-[(*E*)-2-carboxyvinyl]-2-(4-hydroxy-3-methoxyphenyl)-7-methoxy-2,3-dihydro-1-benzofuran-3-carboxylic acid. Molecular formula: $C_{20}H_{18}O_8$. ^{1}H NMR (CD_3OD, 500MHz) δ ppm: 3.66 (s,3H, 1× Ar-OCH_3), 4.2(d,1H, J = 7 Hz), 5.86(d,1H,J = 7 Hz), 6.21 (d,1H,J = 15.5 Hz), 6.5–7.2(m,5H,ArH), 7.47 (d,1H, J = 16.0 Hz). ^{13}C NMR (CD_3OD, 125 MHz) δ ppm: 50.37 (OCH3), 51.54 (OCH3), 55.29, 86.85, 112.22 (ArH), 114.13, 114.69 (olefinic carbon), 115.54 (ArH), 116.39 (ArH), 117.00 (ArH), 125.88, 128.10, 131.35, 141.39, 144.80 (olefinic carbon), 144.99, 145.21, 149.03, 163.84(>C=O), 171.15(.C=O). DEPT: 50.37 (CH_3), 51.54 (CH_3), 55.29 (CH), 86.85 (CH), 112.22 (CH),114.13 (CH), 114.69 (=CH), 115.54 (CH), 116.39 (CH), 117.00 (CH), 125.88 (>C<), 128.10 (>C<), 131.35 (>C<), 141.39 (>C<), 144.80 (=CH 144.99 (>C<), 145.21 (>C<), 149.03 (>C<), 167.84 (>C=O), 171.15(>C=O). The compound was also characterized by mass spectrometry TOF MS ES: 387 (M + H), with purity >93% as determined by high performance liquid chromatography.

Cytotoxicity Assay—Cytotoxicity was assayed by the modified tetrazolium salt 3-(4,5-dimethylthiazol-2-yl)-2,5-diphenyltetrazolium bromide (MTT) assay as described previously (21). Briefly, 5×10^4 cells/well of a 96-well plate were treated with different agents, and the cell viability was determined by incubating the cells with 25 μl of MTT dye (5 mg/ml in PBS) for 4 h at 37 °C. The cells were incubated with 100 μl of lysis buffer (20% SDS in 50% dimethylformamide) overnight at 37 °C, and the absorbance was read at 570 nm.

Cell Cycle Analysis—Cells (log phase culture) were treated with various concentrations of the Benfur. After treatments, the cells were harvested and washed with cold EDTA/PBS (5 mmol/liter) and then suspended in cold EDTA/PBS (300 μl) and 100% chilled ethanol (700 μl), vortexed, and incubated at 37 °C for 1 h. Samples were centrifuged at 200 × *g* for 5 min, and the supernatant was removed. A solution containing propidium iodide (100 μg/ml) and RNase A (1 μg/ml) was added to the samples and incubated for 1 h at 37 °C. Samples were then transferred to 5-ml tubes and analyzed in a flow cytometer (FACS Calibur; Becton Dickinson, San Jose, CA) after gating (FL2-A/FL2-W) the single nuclei population, and data were analyzed using Cell Quest analysis software.

Caspase 3 and 8 Activity Assay—To evaluate caspase 3 and 8 activities, cell extracts were prepared after their respective treatments with the compounds. 50 μg of cell extract protein was incubated with 200 μM caspase 3 substrate (Ac-DVED-pNA) or caspase 8 substrate (Ac-ITED-pNA) in 100-μl reaction buffer (1% Nonidet P-40, 20 mM Tris-HCl, pH 7.5, 137 mM NaCl, and 10% glycerol) and incubated for 2 h at 37 °C. The release of chromophore pNA was monitored spectrophotometrically at 405 nm (21).

Lactate Dehydrogenase (LDH) Release Assay—Necrosis of cells was assayed by measuring LDH, the cytosolic marker, from Benfur-treated cells supernatant. Culture supernatants were incubated with the substrate solution (230 mM sodium pyruvate and 5 mM NADH in 0.1 M phosphate buffer, pH 7.5) and rate of decrease in absorbance at 340 nm was measured.

PARP Cleavage Assay using Flow Cytometry—The PARP cleavage was determined using anti-PARP (85-kDa fragment) antibody (Novus Biologicals) and is used as a marker for detecting apoptotic cells. Treated cells were fixed with chilled 70% ethanol, incubated with 200 μl of permeabilized solution (0.5% bovine serum albumin, 0.02% NaN_3, and 0.5% saponin in PBS) for 30 min at 37 °C, and stained with anti-PARP Ab conjugated with FITC for 1 h. Cells were washed with wash buffer and analyzed in FACS.

Transcription Factor Assay by Electrophoretic Mobility Shift Assay (EMSA)—To determine NF-κB DNA binding activity, EMSA were conducted essentially as described (22). Briefly, 8 μg of nuclear extract proteins were incubated with ^{32}P end-labeled double-stranded NF-κB oligonucleotides for 30 min at 37 °C, and the DNA-protein complex was separated from free oligonucleotide on 6.6% native polyacrylamide gels. Similarly transcription factors like p53, Sp1, and Oct1 DNA binding were assayed using respective ^{32}P end-labeled double-stranded oligonucleotides by EMSA.

NF-κB-dependent Reporter Gene Expression Assay—The NF-κB-dependent reporter gene expression was measured as previously described (22). Briefly, cells were transfected with Qiagen SuperFect reagent with 1 ml of medium containing *p65* plasmid (0.5 μg), *IκBα-DN* (IκBα dominant negative) (0.5 μg), reporter gene of NF-κB promoter DNA linked to the heat-stable secretory alkaline phosphatase (SEAP) (0.5 μg), and GFP (0.5 μg) constructs as described previously by Darnay *et al.* (23). After 3 h of transfection, cells were washed and cultured for 12 h. Cells were visualized under a fluorescent microscope, and 27–30% cells were GFP-positive for different combinations. After different treatments, cell culture-conditioned medium was harvested, and 25 μl of each was analyzed for alkaline phosphatase activity essentially as described by the Clontech protocol (Palo Alto, CA).

Immunocytochemistry—Levels of p21 were examined by the immunocytochemical method as described (24). Briefly, U-937 cells were treated with Benfur and coated in slides, or MCF-7 cells were cultured on poly-L-lysine-coated chamber slides, washed after different treatments, air-dried, fixed with 3.5% formaldehyde, and permeabilized with 0.5% of Triton X-100. Slides were blocked by 5% goat serum, and incubated with anti-p21 Ab for 8 h followed by incubation with goat anti-rabbit IgG-Alexa Fluor for 1 h. Slides were mounted with mounting medium with DAPI and analyzed under a fluorescence microscope.

Study of Molecular Docking—Benfur docking to Sp1 transcription factor was performed with the AutoDock 4.0 program using the empirical free energy function and the Lamarckian genetic algorithm (25). The initial structures of Benfur was designed and optimized in PRODRG server (26). Three-dimensional crystal structures of Sp1 (PDB code 1SP1) (27) (PDB code 1E7A) were used as starting models. The grid maps for whole protein were calculated using an 80 × 80 × 80 points rid size with 0.375Å grid spacing and with an initial population of 300 randomly placed individuals, a maximum number of 2.5×10^7 energy evaluations, a mutation rate of 0.02, a crossover rate of 0.80, and an elitism value of 1, where the average of the worst energy was calculated over a window of the previous 10 generations. For the local search, the so-called Solis and Wets algorithm was applied, using a maximum of 300 interactions. The probability of performing a local search on an individual in the population was 0.06, and the maximum number of consecutive successes or failures before doubling or halving the local search step size was 4 and 100 independent docking runs was carried out for each ligand. Results were clustered according to the 1.0 Å root-mean-square deviation (RMSD) criterions. All torsion angles for each compound were considered flexible. After docking the Benfur-Sp1 complexes were analyzed using PyMol visualization programs (available in the World Wide Web).

RESULTS

Characterization of Benfur—The chemical synthesis of benzofuran derivative is well described under "Experimental Procedures." The chemical structure, mass spectra as well as the NMR data of the novel benzofuran lignan (Benfur) is shown in Fig. 1*A*. We examined its effect on different cell lines. For all experiments, the compound was dissolved in DMSO as 10 mM stock solution, and further dilutions were made in Complete medium.

Benfur-mediated Cell Death Is Cell Type-specific—As cell signaling varies from cell to cell, we incubated Jurkat, U-937, HT29, and MCF-7 cells with different concentrations of Benfur for 72 h, and cell viability was assayed using MTT dye. Cell viability was decreased 60–80% ($p < 0.005$) in Jurkat and MCF-7 cells but 15–20% ($p < 0.001$) in HT29 and U-937 cells (Fig. 1*B*). The 50% growth inhibitory concentration (IC_{50}) of Benfur is about 80 nM at 72 h of incubation for Jurkat cells. Apoptosis was measured by the amounts of cleaved poly(ADP-ribose) polymerase (PARP). Benfur (100 nM) treatment for 24 h showed PARP cleavage almost 40–50% in Jurkat, HeLa, and MCF-7 cells, but only 16% in U-937 cells (Fig. 1*C*). Cell death was observed in Jurkat cells in a time-dependent manner but not in T-cells isolated from fresh human blood (Fig. 1*E*). These data suggest that Benfur-induced cell death is specific for tumor cells. Benfur, at 5,000 and 10,000 nM concentrations increased release of LDH in U-937 and Jurkat cells (Fig. 1*D*), suggesting cytolysis at higher concentrations of Benfur treatments in both cells.

Benfur Increases the Amount of Cytoplasmic Cytochrome c, Cleavage of PARP, Activation of Caspase, and Expression of Bax, but Decreases Bcl-2 Expression—The amounts of cleaved PARP were increased in Benfur-treated Jurkat cells in a concentration- and time-dependent manner as detected through FACS (Fig. 2*A*). The 116-kDa pro-PARP was cleaved to active 85 kDa cleaved PARP in Jurkat cells by the treatment of Benfur in a concentration-dependent manner in Jurkat cells, but not in U-937 cells (Fig. 2*B*). Activity of caspase 3 increased in Benfur-treated cells in a concentration-dependent manner in Jurkat cells, but not in U-937 cells (Fig. 2*C1*). The activity of caspase 8 was not altered in Benfur-treated Jurkat or U-937 cells (Fig. 2*C2*), indicating the effect of Benfur lies more downstream of

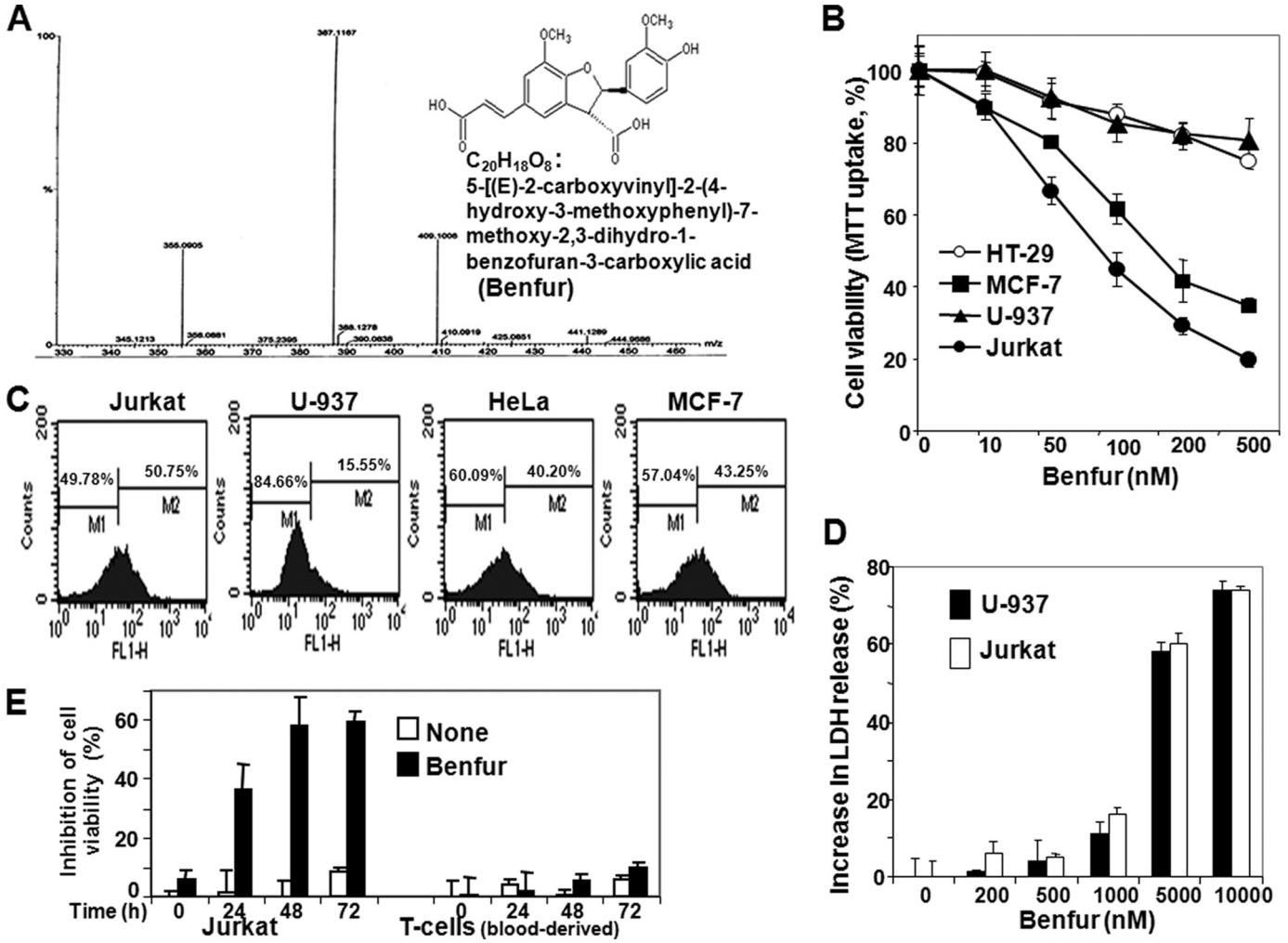

FIGURE 1. **Effect of Benfur on cell death.** The structural formula (5-[(*E*)-2-carboxyvinyl]-2-(4-hydroxy-3-methoxyphenyl)-7-methoxy-2,3-dihydro-1-benzofuran-3-carboxylic acid, designated IUPAC name) (*inset*) and chemical characterization by NMR data for benzofuran lignan (Benfur) are provided (*A*). Jurkat, U-937, HT29, and MCF-7 cells (10,000/well) were treated with different concentrations of Benfur for 24 and 48 h in triplicate. Cell viability was determined by MTT assay and indicated in percentage of cell viability. Error bars indicate ± S.D. *B*, different cells were treated with 100 nM Benfur for 24 h, and the level of apoptosis was measured by incubating cells with FITC-PARP (cleaved fragment) and detected in FACS. Percentage of apoptotic populations are represented as the M2-gated population (*C*). Untreated controls showed an M2 population (*Apoptotic*) between 4–8% (figures are not included here). Jurkat and U-937 cells were treated with different concentrations of Benfur for 48 h in triplicate. The culture supernatant was assayed for LDH and indicated in percentage above untreated cells, considering the 1% Triton X-100-treated cells as 100% (*D*). Jurkat and T-cells (isolated from fresh human blood and purified by nylon wool column) were incubated with 100 nM Benfur for 24 h. Cell viability was measured by MTT assay and indicated as inhibition of cell viability in percentage (*E*).

caspase 8 and may be at the mitochondrial level. The amounts of cytochrome *c* and Bax increased, but Bcl-2 decreased in the cytoplasm as shown by Western blot in Jurkat cells; however they were unaltered in U-937 cells (Fig. 2*D*). All these data suggest that Benfur induces cell death in Jurkat cells, and this effect lies more at the mitochondrial level.

Benfur Blocks Cell Cycle in Jurkat, but Not U-937 Cells—Benfur arrested Jurkat cells in the G2-M phase of the cell cycle (Fig. 2*E1*) leading to significant apoptosis as shown in the sub-G1 content (Fig. 2*E2*). The data shown here confirmed that the concentration of the Benfur (as low as 100 nM) is effective in significant increases (~65%) of the live cells in the G2/M phase of the cell cycle (Fig. 2*E1*). At 50 nM, no significant increase in G2/M population was achieved (data not shown). At 500 nM Benfur, there was further increases in both G2/M and sub-G1 populations (Fig. 2*F*). When U-937 cells were similarly treated with different concentrations of Benfur (upto 500 nM), there was almost no arrest of cells at G2-M phase (Fig. 2*G1*) and also no significant cell death (Fig. 2*G2*). Doxorubicin (100 nM) induced 43 and 45% cell death in Jurkat and U-937 cells, respectively, at 24 h of treatment (data not shown).

Benfur Inhibits DNA Binding Activity of NF-κB and the Dependent Reporter Gene Expression, IκBα Degradation, and p65 Nuclear Translocation—Jurkat and U-937 cells were pretreated with varying concentrations of Benfur for 12 h and then stimulated with 100 ng/ml serum-activated LPS (SA-LPS) for 1 h; nuclear extracts were prepared and assayed for NF-κB by gel shift assay. Benfur inhibited SA-LPS-induced NF-κB DNA binding activity in a dose-dependent manner in both cells (Fig. 3*A*). Benfur inhibited SA-LPS-induced expression of NF-κB dependent reporter gene SEAP in the NF-κB SEAP reporter construct transfected in both Jurkat and U-937 cells (Fig. 3*B*). To determine whether the inhibitory action of Benfur was due to inhibition of IκBα degradation mediated by SA-LPS,

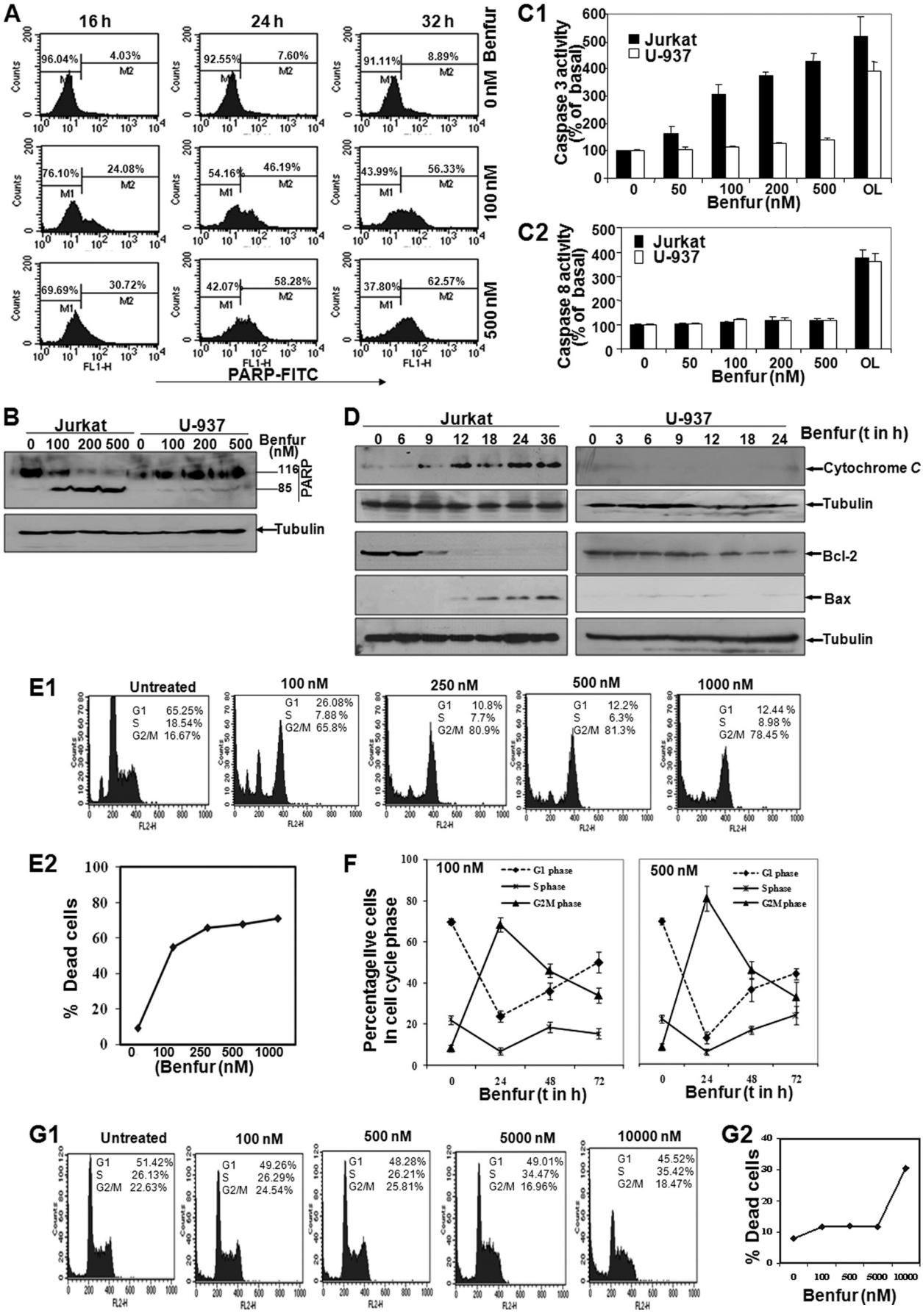

IκBα proteins was measured from cytoplasmic extracts (CE), and p65 was measured from nuclear extracts (NE). IκBα degradation started at 1 h of SA-LPS (100 ng/ml) treatment in cells. Benfur-pretreated cells showed inhibition of SA-LPS-induced IκBα degradation (Fig. 3*C*, *upper left & right panels*). In SA-LPS-stimulated Jurkat and U-937 cells, the amount of p65 decreased in the CE at 1 and 2 h and increased in the NE at the same time points. Benfur-pretreated cells showed that high amounts of p65 were in CE, but not in NE (Fig. 3*C*, *middle & lower* and *left & right panels*).

Benfur Partially Induces Cell Death in NF-κB-expressing Cells—Jurkat and U-937 cells (transfected with vector alone or *p65* constructs) were incubated with varying concentrations of Benfur for 12 h. The *p65*-transfected cells showed high amounts of NF-κB DNA binding activity in nuclear extracts (Fig. 3*D*). Jurkat and U-937 cells (transfected with vector alone, *p65,* or IκBα-DN constructs) were treated with 100 nM Benfur for 24 h, and cell viability was measured by MTT assay. Benfur induced cell death 50% in vector-transfected, 30% in p65-transfected, and 80% in IκBα-DN-transfected Jurkat cells. The 40% cell death was observed in IκBα-DN-transfected cells (Fig. 4*E*, *left panel*). Benfur induced 20% cell death in vector-transfected U-937 cells. No cell death was observed in p65-transfected U-937 cells by Benfur treatment. Like Jurkat cells, 40% cells death was observed in IκBα-DN-transfected U-937 cells, which was not further enhanced by Benfur treatment (Fig. 3*E*, *right panel*). These data suggest that partial cell death was observed due to inhibition of NF-κB in Jurkat cells, whereas the 15–20% cell death, which was observed by Benfur in U-937 cells is due to inhibition of NF-κB.

Primary T-cells, isolated from fresh human blood, showed high basal NF-κB DNA binding. Benfur did not decrease NF-κB DNA binding in primary T-cells, but decreased in serum-activated Jurkat cells (Fig. 3*F*). These results suggest that Benfur is ineffective in primary cells.

Benfur Increases p53 DNA Binding Activity and Amounts of p21 and p27 in Jurkat and U-937 Cells—To understand the difference between Benfur-sensitive *versus* -resistant cells, we treated U-937 and Jurkat cells with different concentrations of Benfur for 12 h, and the nuclear extracts were used to measure p53 by gel shift assay. U-937 cells showed very low basal p53 DNA binding compared with Jurkat cells. Benfur treatment increased p53 DNA binding in Jurkat cells at 200 nM concentration (Fig. 4*A*). The amounts of p21, p27, or cyclin B, but not phospho-Rb or Rb were increased with increasing concentrations of Benfur as shown by Western blot from whole cell extracts (Fig. 4*B*). The amount of p21 was also increased in MCF-7 cells upon treatment of Benfur as shown by immunofluorescence technique (Fig. 4*C*). These data suggest that p53 might have a role in Benfur-mediated cell signaling. To confirm further the role of Benfur on p53-mediated induction of cell death, p53-stably transfected HCT116 ($p53^{+/+}$) cells were treated with different concentrations of Benfur, and cell viability was assayed by MTT dye uptake. Benfur treatment did not alter high basal amounts of p53 as shown by Western blot (Fig. 4*D*). HCT116 cells showed only 10–15% cell death at 100–200 nM Benfur, whereas in p53-positive cells Benfur induced cell death with increasing concentrations (Fig. 4*E*). These data further suggest that Benfur-mediated apoptosis is p53-dependent.

Benfur Decreases Amounts of MDM2 and p53 and DNA Binding to Sp1 in Jurkat Cells—To understand the mechanism of Benfur-mediated increases in p53 DNA binding activity, we treated U-937 and Jurkat cells with 100 nM Benfur for different times. The amount of MDM2 as measured by RT-PCR decreased with the increasing time of Benfur treatment in Jurkat, but not in U-937 cells (Fig. 5*A*). The expression of MDM2 decreased, and the p53 increased with the increasing time of Benfur treatment in Jurkat, but not in U-937 cells (Fig. 5*B*). As MDM2 expression is regulated by Sp1 transcription factor, we have measured the Sp1 upon similar treatment conditions. The Sp1 DNA binding activity decreased in Jurkat cells with increasing time of Benfur treatment without interfering in Oct1 DNA binding (Fig. 5*C*). The Sp1 DNA binding activity decreased *in vitro* upon Benfur treatment (Fig. 5*D*). The Benfur binds to Sp1 catalytic amino acids Lys^{29}, Gln^{20}, and Glu^{07} (Fig. 5*E*). Results were obtained under 298.15 K temperatures with solvation of water molecule as the solvent parameter. AutoDock binding affinities of the Benfur, evaluated by free energies (ΔGb, kcal/mol), inhibition constants (K_i), hydrogen bonds, and RMSD values. The obtained success rates of AutoDock is high, where the docked Benfur binding energies is −13.42 kcal/mol at 1.21 Å RMSD (Table 1), and predicted hydrogen bonds form inbetween the Lys^{29}, Gln^{20}, and Glu^{07} of Sp1 and Benfur. These data suggest that Benfur inhibits Sp1 transcription factor thereby decreases the amount of MDM2 and thus increases the amount of p53.

DISCUSSION

Chemoprevention is considered a promising strategy in the field of cancer therapy and suppressing or reversing the process of tumor formation has gained much attention (28, 29). Classic cytotoxic agents, known to act on the cell cycle, continue to

FIGURE 2. **Effect of Benfur on PARP cleavage, caspase activity, cell cycle stages, and amounts of cytoplasmic cytochrome *c*, Bax, and Bcl-2.** Jurkat cells were treated with 100 and 500 nM Benfur for the indicated time period, and PARP cleavage was determined using FACS analysis as described under "Experimental Procedures." Percentage apoptotic populations are represented as the M2-gated population (*A*). Jurkat and U-937 cells were treated with different concentrations of Benfur for 48 h, and then PARP was detected from whole cell extracts by Western blot (*B*). Jurkat cells were treated with indicated concentrations of the compound for 24 h and harvested in lysis buffer. Cellular lysates were incubated with caspase 3 substrate (Ac-DVED-pNA) (*C1*) or caspase 8 substrate (Ac-ITED-pNA) (*C2*), and absorbance was recorded at 405 nm. Results are presented as percentage of caspase activities considering 100% for untreated cells. Oleandrin (*OL*) (100 ng/ml) was used to treat the cells as a positive control. Jurkat and U-937 cells were treated with 100 nM Benfur for variable times, and the amounts of cytochrome *c*, Bax, and Bcl-2 were measured from cytoplasmic extracts by Western blot (*D*). Jurkat (5×10^5) cells were treated with different concentrations of Benfur for 24 h and after staining with PI, cell cycle distribution was analyzed using a flow cytometer. The data indicate the percentage of live cell population in each phase of the cell cycle (*E1*). All experiments were performed in duplicate and showed similar results. The percentage apoptotic population is depicted in the graph (*E2*). Jurkat cells were treated with 100 and 500 nM Benfur for 24, 48, and 72 h in triplicate, and the percentage live population in the cell cycle phases (G1, S, and G2/M) were analyzed by flow cytometry (*F*). U-937 (5×10^5) cells were treated with different concentrations of the Benfur for 24 h and after staining with PI, cell cycle distribution was analyzed using a flow cytometer. Data indicate the percentage of live cell population in each phase of the cell cycle (*G1*). All experiments were performed in duplicate and gave similar results. The percentage apoptotic population is depicted in the graph (*G2*).

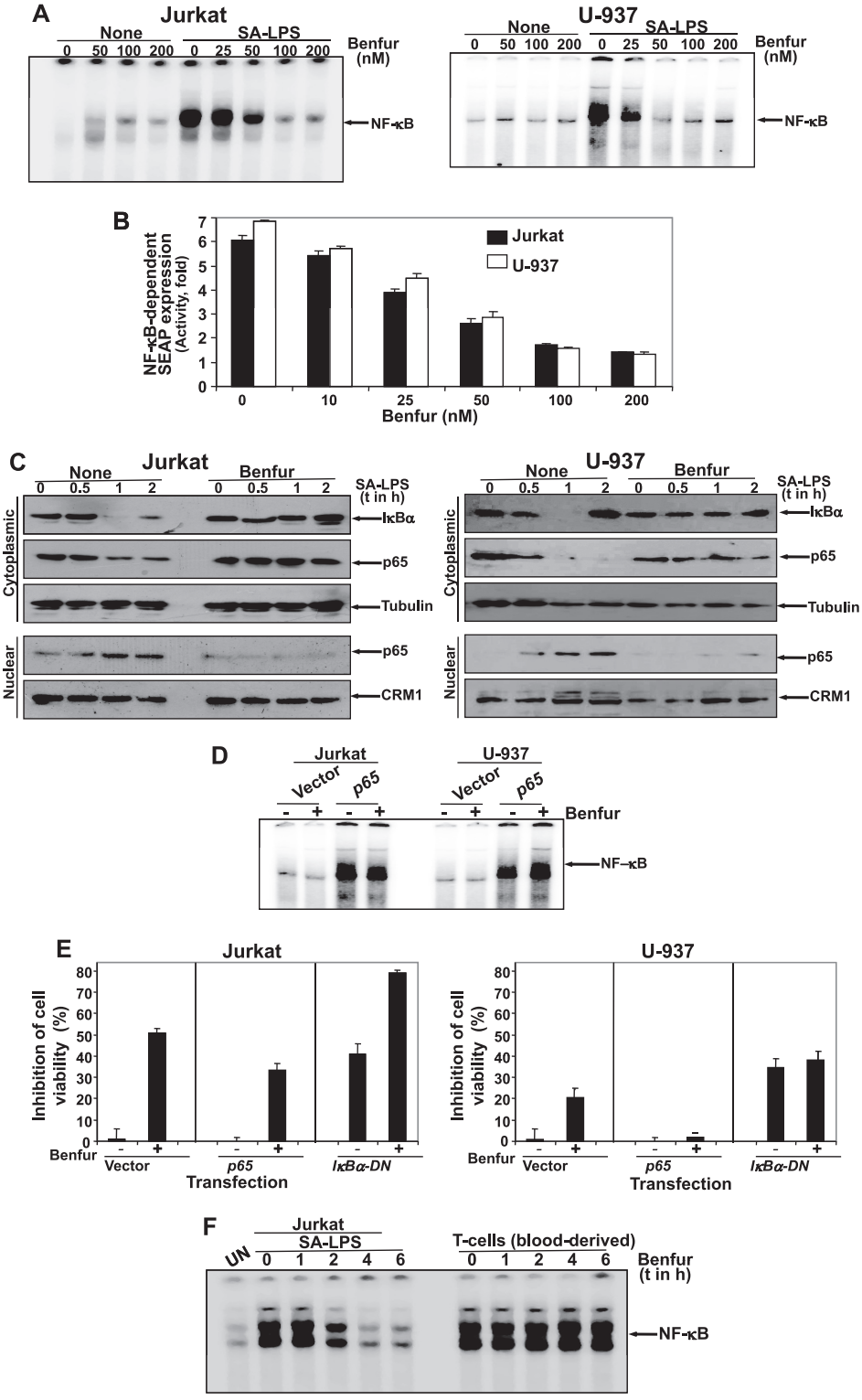

FIGURE 3. **Effect of Benfur on SA-LPS-induced activation of NF-κB and nuclear translocation of p65.** Jurkat and U-937 cells were treated with different concentrations of Benfur for 12 h and then stimulated with 100 ng/ml SA-LPS for 1 h. Nuclear extracts were prepared and used for NF-κB DNA binding (*A*). Jurkat and U-937 cells were transiently transfected with an NF-κB containing plasmid linked to the *SEAP* gene. After 12 h, cells were treated with different concentrations of Benfur for 12 h and then stimulated with 100 ng/ml SA-LPS for 6 h. Cell culture-conditioned medium was harvested and assayed for SEAP activity as described in the Clontech Great EscApe SEAP protocol. Results are expressed as fold activity over the nontransfected control value. Transfection efficiency was analyzed with *pEGFP-N1* (Clontech) control vector (*B*). Jurkat and U-937 cells, pretreated with Benfur (100 nM) for 12 h were stimulated with 100 ng/ml SA-LPS for different times. Cytoplasmic extracts were used to measure the amount of IκBα, and the same blot was reprobed for p65 and tubulin. Nuclear extracts were used to measure p65 by Western blot (*C*). Jurkat and U-937 cells were transfected with *p65* and *NF-κB-SEAP* reporter constructs for 3 h with Lipofectamine. Cells were cultured for 12 h and then treated with different concentrations of Benfur for 12 h. Nuclear extracts were used to measured NF-κB DNA binding (*D*). Jurkat and U-937 cells (vector, *p65*-transfected, or IκBα-DN (dominant negative IκBα) transfected for 3 h and then cultured for 12 h) were treated without or with 100 nM Benfur for 24 h. Cell viability was assayed by MTT assay and indicated as inhibition of cell viability in percentage (*E*). Jurkat cells and T-cells (isolated from fresh human blood by Ficoll-hypaque followed by nylon wool column methods) were treated with 100 nM Benfur for different times. NF-κB was assayed from nuclear extracts (*F*).

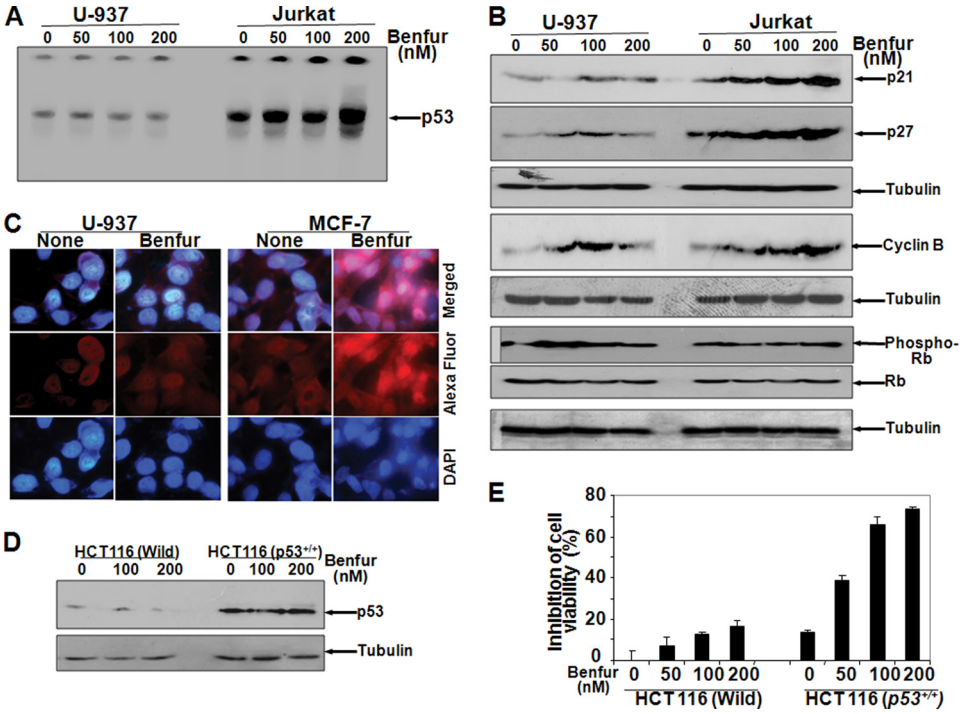

FIGURE 4. **Effect of Benfur on the amounts of p53, p21, p27, cyclin B, and retinoblastoma.** U-937 and Jurkat cells were treated with different concentrations of Benfur for 12 h. The p53 DNA binding was detected from nuclear extracts by gel shift assay (*A*). The amounts of p21, p27, cyclin B, phospho-Rb, and Rb were measured from 100 μg of whole cell extracts by Western blot (*B*). All those blots were reprobed for tubulin. U-937 and MCF-7 cells were treated with Benfur (100 nM) for 12 h, and cells were used to measure p21 by immunofluorescence microscope (*C*). HCT116 and p53 stably transfected [HCT116 ($p53^{+/+}$)] cells were treated with different concentrations of Benfur for 48 h. The amount of p53 was measured by Western blot (*D*), and cell viability was assayed by MTT assay and indicated as inhibition of cell viability in percentage (*E*).

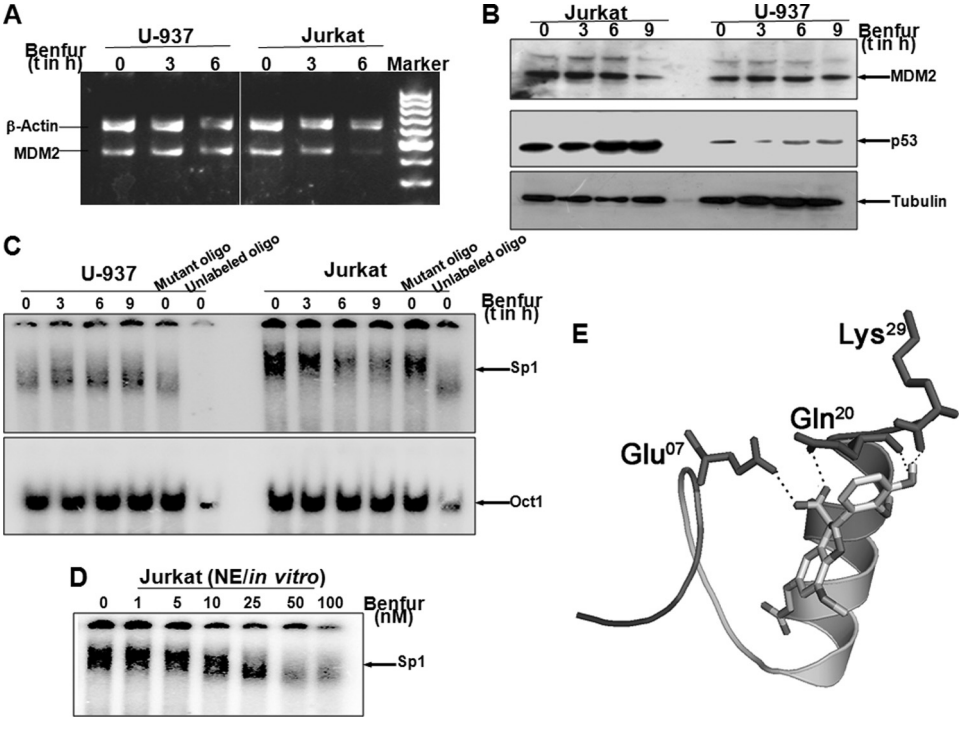

FIGURE 5. **Effect of Benfur on the amount of MDM2 and Sp1 DNA binding.** U-937 and Jurkat cells were treated with Benfur (100 nM) for different times. The amounts of MDM2 and actin were detected by RT-PCR followed by PCR from total RNA (*A*). The amounts of MDM2 and p53 were measured from whole cell extracts by Western blot (*B*). The DNA binding to Sp1 and Oct1 was detected from nuclear extracts by gel shift assay (*C*). Nuclear extracts from Jurkat cells were incubated with different concentrations of Benfur for 2 h, and Sp1 DNA binding was carried out by gel shift assay (*D*). Docking interaction of Benfur with Sp1 transcription factor (PDB ID: 1SP1) was performed with the AutoDock 4.0 program (*E*).

underline first line treatments in oncology. Therefore, novel targeted therapeutics, especially, those modulating the G2/M cell cycle checkpoint have emerged as an attractive candidate for new cancer therapies (30).

Some of the derivatives of benzofuran lignan were found to act against tumor proliferation (19, 31). We provided evidence that a novel synthetic benzofuran lignan (known as Benfur) induced cell death by G2/M phase arrest in $p53^{+/+}$ cells at low concentration. Benfur was able to inhibit cell growth in specific cell types. Molecules involved in cell signaling that lead to cell growth vary from cell to cell. The cells that have high p53 expression were affected at low concentrations of Benfur. It inhibited cell growth in a dose-dependent manner with an IC_{50} value of around 80 nM in Jurkat cells, known to be $p53^{+/+}$ cells (32). Flow cytometric analysis of DNA content showed a dose-dependent block in the G2/M phase and an increase in the sub-G1 (apoptotic) cell population. At 100 nM concentration, almost 66% of the live population were arrested in the G2/M phase and around 54% of the total population appeared in the sub-G1 (apoptotic) state in Jurkat cells. Furthermore the effect of the G2/M promoting doses of the compound was time-dependent with maximal arrest at 24 h. Though in the lower concentrations of Benfur only 10–20% cell death was observed in U-937 cells, at higher concentrations, it induced cell death in U-937 cells by increasing marginal S phase population followed by apoptosis. Though at higher concentrations of Benfur, both cells showed necrosis, how it induces S-phase arrest in U-937 cells should be studied. Activation of the *p53* gene (tumor suppressor) is known to play a role in the regulation of cell cycle arrest at G2/M phase (9, 10). The high basal expression of p53 was observed in Jurkat than U-937 cells. However, U-937 cells lack the *p53* protein because of a 46-base deletion mutation in the *p53* gene (33). Benfur

TABLE 1
Docking score of Benfur with Sp1 transcription factor

Protein	Ligand	Cluster rank	RMSD[a]	Lowest energy of binding[b]	Inhibition constant (K_i)
				kcal/mol	μM
Sp1 (Transcription factor)	Benfur	1	1.21	−13.42	$+1.14e^{-05}$
		2	1.84	−7.24	$+4.15^{-05}$
		3	1.09	−7.32	$+4.97^{-05}$
		4	1.65	−6.45	$+5.25^{-05}$
		5	1.29	−6.69	$+5.75^{-05}$

[a] RMSD of best docked conformation with respect to the reference conformation.
[b] Lowest binding energy = intermolecular energy + total internal energy + torsional free energy − unbound system's energy.

increased p53 DNA binding activity and its dependent p21 and p27 genes. Cyclin B has shown to degrade in G2/M phase of cell cycle (34). Increased amounts of cyclin B were decreased at higher concentrations of Benfur treatment in U-937, but not in Jurkat cells, suggesting G2/M phase arrest only in Jurkat cells. Benfur possibly affects mitochondrial events that lead to release of cytochrome *c* followed by activation of caspase 3. Activation of caspase 8, an upstream of mitochondrial event, was not affected by Benfur treatment.

NF-κB regulates cell cycle by expressing several NF-κB-dependent genes and also induces cell proliferation. Benfur potentially inhibits NF-κB DNA binding activity by inhibiting IκBα (inhibitory subunit of NF-κB) and thereby nuclear translocation of p65 (subunit of NF-κB) in both Jurkat and U-937 cells. IκBα degradation is preceded by phosphorylation by IκBα kinase complex (IKKs), and this may be the target of action. Activation of NF-κB exerts both pro- and anti-apoptotic activities through expression of its dependent genes (35). NF-κB-expressing cells are known to be resistant to cell death (22, 36–38). Alone Benfur showed almost 50% cell death. Surprisingly, NF-κB-expressing (*p65*-transfected) cells showed only 35% apoptosis, which suggests that Benfur-mediated cell death occurs mostly through the non-NF-κB pathway. In Jurkat cells, Benfur was shown to induce cell death by 10–20% and that was due to inhibition of NF-κB, as Benfur did not induce cell death in NF-κB-expressing U-937 cells or did not potentiate cell death in null/low NF-κB-expressing (IκBα-DN-transfected) cells.

As Benfur inhibited MDM2 expression in $p53^{+ve}$ cells and MDM2 also activates p65 via the Sp1 transcription factor, Benfur has a role in down-regulating NF-κB via decreasing MDM2 that leads to cell death. *In silico* data suggest that Benfur strongly binds with Sp1 and represses its dependent gene MDM2 expression. Low amounts of MDM2 thus stabilize p53, which might be important for Benfur-mediated cell death in p53-positive cells. NF-κB down-regulated (IκBα-DN-transfected) cells showed almost 40% cell death, and this increased to 75% with Benfur treatment. Decreases in the basal expression of NF-κB-dependent genes drives cells to cell death and inhibits the proliferative effect. These data suggest that in low or null NF-κB-expressing cells, Benfur induced an additive cell death effect. The expression of p53 is dependent upon MDM2. MDM2 again negatively regulates p53 by activating ubiquitin-mediated degradation of p53. Benfur treatment was shown to increase p53 DNA binding, which is correlated with the decrease in the amount of MDM2 and Sp1 DNA binding. The Sp1 DNA binding is directly inhibited by Benfur. So, Benfur-mediated repression of Sp1 might lead to inhibition of MDM2 expression and that causes increase in the amount of p53. Decreases in the amount of MDM2 again inhibit NF-κB activation via blocking of p65 expression. Thus, Benfur-mediated decreases in MDM2 might have a double-sword effect to induce cell death via expression of p53 (39) and inhibition of NF-κB (16). Benfur treatment decreased NF-κB DNA binding and induced cell death in Jurkat cells, but not in primary T-cells isolated from blood, a striking effect of Benfur. Tumor cells are more aggressive in the uptake of the nutrients from medium than primary cells, and this property may be a possible way to uptake Benfur from medium to show its effect in tumor cells.

Overall, our data indicate a correlation between the G2/M arrest and an induction of apoptosis in response to the treatment with novel benzofuran lignan of Jurkat cells. The influence of the compound is cell type-specific. At lower concentrations, no arrest in the G2/M phase was seen in the case of p53-negative or mutant cells, but partial cell death was observed due to inhibition of NF-κB. Taken together, this may indicate that there are two independent mechanisms, *p53*-dependent and *p53*-independent, occurring in the examined cell lines at different doses. Possibly *p53* function is required to observe a maximum response to the compound exerted via G2/M cell cycle arrest and induction of apoptosis. Thus, this novel derivative of benzofuran may be a promising anticancer drug alone or in combination with other drugs that need further validation by *in vivo* study.

Acknowledgments—We thank Dr. J. V. Raman, Research Director and Head, Chemical Research Technology Group, Reliance Life Sciences and Prof. T. Ramasarma, Hon. Distinguished Chair, CDFD, Hyderabad for valuable comments on the work.

REFERENCES

1. Perez-Stable, C. (2006) *Cancer Lett.* **231,** 49–64
2. Li, Q., Sham, H., and Rosenberg, S. (1999) *Annual Reports in Medicinal Chemistry*, Vol. 34, pp. 139–148, Academic Press Inc., New York
3. Jordan, A., Hadfield, J. A., Lawrence, N. J., and McGown, A. T. (1998) *Med. Res. Rev.* **18,** 259–296
4. Concin, N., Stimpfl, M., Zeillinger, C., Wolff, U., Hefler, L., Sedlak, J., Leodolter, S., and Zeillinger, R. (2003) *Int. J. Oncol.* **22,** 51–57
5. Takizawa, C. G., and Morgan, D. O. (2000) *Curr. Opin. Cell Biol.* **12,** 658–665
6. Hale, A. J., Smith, C. A., Sutherland, L. C., Stoneman, V. E., Longthorne, V. L., Culhane, A. C., and Williams, G. T. (1996) *Eur. J. Biochem.* **236,** 1–26
7. Basu, A., and Haldar, S. (1998) *Mol. Hum. Reprod.* **4,** 1099–1109
8. Gangadharan, C., Thoh, M., and Manna, S. K. (2010) *Breast Cancer Res. Treat.* **120,** 671–683
9. Stewart, N., Hicks, G. G., Paraskevas, F., and Mowat, M. (1995) *Oncogene* **10,** 109–115
10. Taylor, W. R., and Stark, G. R. (2001) *Oncogene* **20,** 1803–1815
11. Bunz, F., Dutriaux, A., Lengauer, C., Waldman, T., Zhou, S., Brown, J. P., Sedivy, J. M., Kinzler, K. W., and Vogelstein, B. (1998) *Science* **282,** 1497–1501
12. Piette, J., Neel, H., and Maréchal, V. (1997) *Oncogene* **15,** 1001–1010
13. Bond, G. L., Hu, W., Bond, E. E., Robins, H., Lutzker, S. G., Arva, N. C., Bargonetti, J., Bartel, F., Taubert, H., Wuerl, P., Onel, K., Yip, L., Hwang, S. J., Strong, L. C., Lozano, G., and Levine, A. J. (2004) *Cell* **119,** 591–602
14. Kaku, S., Iwahashi, Y., Kuraishi, A., Albor, A., Yamagishi, T., Nakaike, S., and Kulesz-Martin, M. (2001) *Nucleic Acids Res.* **29,** 1989–1993
15. Chène, P. (2004) *Mol. Cancer Res.* **2,** 20–28

16. Gu, L., Findley, H. W., and Zhou, M. (2002) *Blood* **99,** 3367–3375
17. Pieters, L., de Bruyne, T., Claeys, M., Vlietinck, A., Calomme, M., and vanden Berghe, D. (1993) *J. Nat. Prod.* **56,** 899–906
18. Hansott, B., Greger, H., and Marian, B. (2003) *J. Cancer Res. Clin. Oncol.* **129,** 569–576
19. Pieters, L., Dyck, S. V., Gao, M., Bai, R., Hamel, E., Vlietinck, A., and Lemière, G. (1999) *J. Med. Chem.* **42,** 5475–5481
20. Trizio, D., and Cudkowicz, G. (1974) *J. Immunol.* **113,** 1093–1097
21. Raghavendra, P. B., Sreenivasan, Y., Ramesh, G. T., and Manna, S. K. (2007) *Apoptosis* **12,** 307–318
22. Manna, S. K., Manna, P., and Sarkar, A. (2007) *Cell Death Diff.* **14,** 158–170
23. Darnay, B. G., Ni, J., Moore, P. A., and Aggarwal, B. B. (1999) *J. Biol. Chem.* **274,** 7724–7731
24. Manna, S. K., and Gangadharan, C. (2009) *Mol. Immunol.* **46,** 1340–1350
25. Morris, G. M., Goodsell, D. S., Halliday, R. S., Huey, R., Hart, W. E., Belew, R. K., and Olson, A. J. (1998) *J. Comput. Chem.* **19,** 1639–1662
26. Schuettelkopf, A. W., and van Aalten, D. M. F. (2004) *Acta Crystallogr. D* **60,** 1355–1363
27. Narayan, V. A., Kriwacki, R. W., and Caradonna, J. P. (1997) *J. Biol. Chem.* **272,** 7801–7809
28. Aggarwal, B. B., Takada, Y., and Oommen, O. V. (2004) *Exp. Opin. Invest. Drugs* **13,** 1327–1338
29. Levi, M. S., Borne, R. F., and Williamson, J. S. (2001) *Curr. Med. Chem.* **8,** 1349–1362
30. Potter, A. J., Gollahon, K. A., Palanca, B. J., Harbert, M. J., Choi, Y. M., Moskovitz, A. H., Potter, J. D., and Rabinovitch, P. S. (2002) *Carcinogenesis* **23,** 389–401
31. Apers, S., Paper, D., Bürgermeister, J., Baronikova, S., Van Dyck, S., Lemière, G., Vlietinck, A., and Pieters, L. (2002) *J. Nat. Prod.* **65,** 718–720
32. Mansilla, S., Piña, B., and Portugal, J. (2003) *Biochem. J.* **372,** 703–711
33. Sugimoto, K., Toyoshima, H., Sakai, R., Miyagawa, K., Hagiwara, K., Ishikawa, F., Takaku, F., Yazaki, Y., and Hirai, H. (1992) *Blood* **79,** 2378–2383
34. Dash, B. C., and El-Deiry, W. S. (2005) *Mol. Cell Biol.* **25,** 3364–3387
35. Pöppelmann, B., Klimmek, K., Strozyk, E., Voss, R., Schwarz, T., and Kulms, D. (2005) *J. Biol. Chem.* **280,** 15635–15643
36. Manna, S. K., Babajan, B., Raghavendra, P. B., Raviprakash, N., and Sureshkumar, C. S. (2010) *J. Biol. Chem.* **285,** 11617–11627
37. Gangadharan, C., Thoh, M., and Manna, S. K. (2009) *J. Cell. Biochem.* **107,** 203–213
38. Sreenivasan, Y., Sarkar, A., and Manna, S. K. (2003) *Oncogene.* **22,** 4356–4369
39. Chen, H. W., and Huang, H. C. (1998) *Br. J. Pharmacol.* **124,** 1029–1040

Signal Transduction:

Novel Derivative of Benzofuran Induces Cell Death Mostly by G2/M Cell Cycle Arrest through p53-dependent Pathway but Partially by Inhibition of NF- κB

Sunil K. Manna, Julie S. Bose, Vijay Gangan, Nune Raviprakash, Thota Navaneetha, Pongali B. Raghavendra, Banaganapalli Babajan, Chitta S. Kumar and Swatantra K. Jain

J. Biol. Chem. 2010, 285:22318-22327.
doi: 10.1074/jbc.M110.131797 originally published online May 14, 2010